

Synthesis and Evaluation of Novel α -Fluorinated (*E*)-3-((6-Methylpyridin-2-yl)ethynyl)cyclohex-2-enone-*O*-methyl Oxime (ABP688) Derivatives as Metabotropic Glutamate Receptor Subtype 5 PET Radiotracers

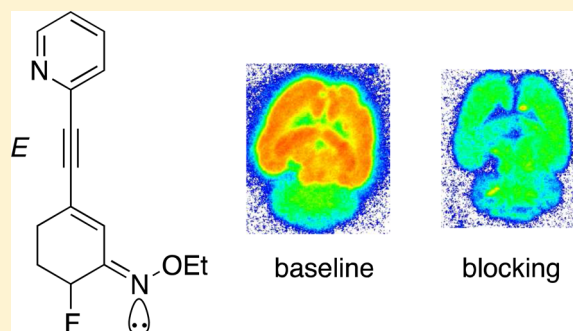
Selena Milicevic Sephton,[†] Linjing Mu,[†] W. Bernd Schweizer,[‡] Roger Schibli,[†] Stefanie D. Krämer,[†] and Simon M. Ametamey^{*,†}

[†]Center for Radiopharmaceutical Sciences of ETH, PSI and USZ, Department of Chemistry and Applied Biosciences, Swiss Federal Institute of Technology (ETH) Zurich, Wolfgang-Pauli Strasse 10, 8093, Zurich, Switzerland

[‡]Laboratory of Organic Chemistry, Department of Chemistry and Applied Biosciences, Swiss Federal Institute of Technology (ETH) Zurich, Wolfgang-Pauli Strasse 10, 8093 Zurich, Switzerland

S Supporting Information

ABSTRACT: In the search for an optimal fluorine-18-labeled positron emission tomography (PET) radiotracer for imaging metabotropic glutamate receptor subtype 5 (mGluR5), we have prepared a series of five α -fluorinated derivatives based on the ABP688 structural manifold by application of a two-step enolization/NFSI α -fluorination method. Their binding affinities were evaluated in vitro, and the most promising candidate (*Z*)-**16** exhibited a K_i of 5.7 nM and a $\log P$ value of 2.3. The synthesis of the precursor tosylate (*E*)-**22** revealed a preference for the (*E*)-configurational isomer ($K_i = 31.2$ nM), and successful radiosynthesis afforded (*E*)-[¹⁸F]-**16** which was used as a model PET tracer to establish plasma and PBS stability. (*E*)-[¹⁸F]-**16** ($K_d = 70$ nM) exhibited excellent specificity for mGluR5 in autoradiographic studies on horizontal rat brain slices in vitro.



INTRODUCTION

Positron emission tomography (PET) is a noninvasive imaging technique in which 3D concentration images are obtained through computational analysis of pairs of γ rays emitted indirectly from compounds containing positron emitting nuclides such as [¹¹C] or [¹⁸F].^{1–3} Metabotropic glutamate receptor subtype 5 (mGluR5) is a G-protein-coupled postsynaptic receptor, and it belongs to group I of metabotropic glutamate receptors, which together with ionotropic glutamate receptors regulate glutamate, a major excitatory neurotransmitter in mammalian brain.^{4–8} In 2006, the Ametamey group reported on the synthesis, radiolabeling, and pharmacological evaluation of [¹¹C]-**1** ([¹¹C]-ABP688, Figure 1) and subsequently illustrated its application as a PET radiotracer for imaging of mGluR5 in vivo in human subjects.^{9–11} The success of this first mGluR5 PET tracer was immediate, and [¹¹C]-**1** was employed in many clinical studies^{12–19} particularly because mGluR5 emerged as an important drug target due to its demonstrated involvement in long-term potentiation processes as well as several CNS disorders²⁰ (e.g., schizophrenia,²¹ depression,²² neuropathic pain,^{23,24} drug addiction,²⁵ Fragile X syndrome,²⁶ and Alzheimer's^{19,27} and Parkinson's disease^{28,29}). Although clinically applied with success, [¹¹C]-**1** has one significant limitation

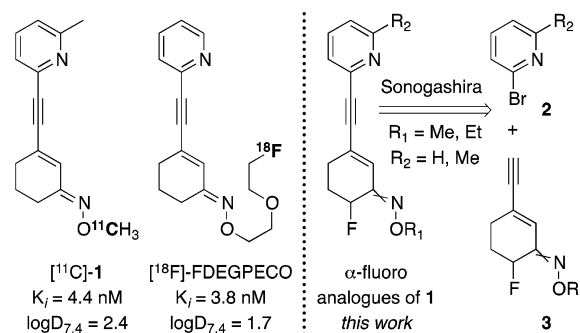


Figure 1. Structures of carbon-11 and fluorine-18 mGluR5 PET radiotracers from the Ametamey group and the synthetic plan to a new series of α -fluorinated analogues of **1**. A crossed double bond is used to indicate double bond isomers (*E* and *Z*).

which is the short physical half-life (20 min) of the carbon-11 nuclide that limits its application to facilities with an on-site cyclotron. This opened the possibility for further advancement of mGluR5 PET tracers with the aim of designing a fluorine-18-labeled tracer.

Received: May 9, 2012

Published: July 23, 2012

Fluorine-18 has a longer physical half-life (110 min) and, to date, two of the most successful mGluR5 ^{18}F -labeled PET tracers are 3-fluoro-5-(2-([^{18}F](fluoromethyl)thiazol-4-yl)ethynyl)benzonitrile ([^{18}F]-SP203), developed by the Pike group,^{30–32} which showed limited defluorination in human subjects, and 3-[^{18}F]fluoro-5-(2-pyridinylethynyl)benzonitrile ([^{18}F]-FPFB), developed by the Hamill group^{33,34} which has also been applied in human subjects but is typically obtained in low radiochemical yields. Neither Pike's nor Hamill's analogues were based on the structural scaffold of **1**, and the success of [^{11}C]-**1** in human clinical practice prompted us to explore close analogues of [^{11}C]-**1**. Among other evaluated fluorinated radiotracers^{35–39} to date, (*E*)-3-(pyridin-2-ylethynyl)cyclohex-2-enone *O*-(2-(2-[^{18}F]fluoroethoxy)ethyl) oxime ([^{18}F]-FDEGPECO, Figure 1)^{40,41} was identified as the most promising candidate, which was successful in visualizing mGluR5 *in vivo* in a rat brain without defluorination, albeit with relatively high background activity.

Taking advantage of the success of [^{11}C]-**1** while incorporating fluorine-18 with the more desirable physical half-life, we aimed to investigate structures most closely related to [^{11}C]-**1**, in which a hydrogen atom is replaced by fluorine. Apart from increasing the physical half-life of the radiotracer, incorporation of a fluorine atom also alters chemical and physical properties of the molecule particularly with respect to the lipophilicity of the molecule, mainly due to the electronegativity of the fluorine atom.^{42–44} Fluorine-containing molecules typically show increased log *D* when compared to their nonfluorinated analogues,⁴⁵ and this is favorable for the development of CNS tracers, as it typically allows greater permeation of the blood–brain barrier. On the basis of the ease of their synthetic accessibility as well as their optimal clog*P* values such that they are in the range of that of [^{11}C]-**1** (2.4), we designed a series of α -fluoro-substituted compounds (Figure 1) and herein we report on their chemical syntheses, structural elucidation, and determination of binding affinities, as well as the establishment of the model PET radiotracer and evaluation of its *in vitro* properties.

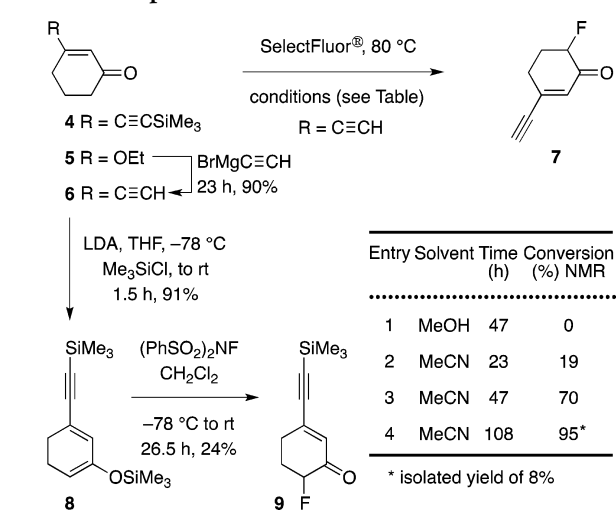
RESULTS AND DISCUSSION

The synthesis of α -fluoro [^{11}C]-**1** derivatives was envisioned via the Sonogashira cross-coupling of α -fluoro oxime ether **3** and corresponding bromopyridines (**2**) as depicted in Figure 1.

Ethylene enone **6** (Scheme 1) was prepared by reacting commercially available ethoxy enone **5** with ethynylmagnesium bromide. In order to obtain α -fluoroenone **7**, enone **6** was treated with SelectFluor following the procedure reported by Zupan and co-workers.^{46,47} While in methanol **6** was completely unreactive, in acetonitrile a 19% conversion was determined by NMR (entry 1 vs entry 2, Scheme 1). With longer reaction times, conversion to **7** was significantly improved (entries 2–4); however, purification by chromatography on a silica gel column afforded only 8% of α -fluoroenone **7**.

Alternatively, α -fluorination was accomplished via a two-step procedure. In the first step, enone **6** was enolized with LDA and quenched with chlorotrimethylsilane⁴⁸ to afford TMS-enol ether **8** with the concurrent protection of the free acetylene in **6**. Silyl enol ether **8** was then fluorinated using *N*-fluorobenzenesulfonimide (NFSI) in 24% yield, which could not be improved regardless of the duration or temperature of the reaction. Application of a two-step protocol enolization/NFSI α -fluorination has been accomplished with ketones,

Scheme 1. Optimization of α -Fluorination of Enone **6**



giving rise to related products in low yields requiring long reaction times.⁴⁹ To our knowledge, γ -fluorination⁵⁰ was the only application of NFSI with unsaturated ketones in which case enolization was achieved using triphenylborane.

Recently, the MacMillan group and others described advanced applications of NFSI for asymmetric α -fluorination of aldehydes^{51–53} and ketones⁵⁴ in excellent yields and high enantioselectivity. In our hands, the enantioselective α -fluorination of **4** under MacMillan's reaction conditions produced *ent*-**9** in 8% yield and 94% ee. Our initial pharmacological evaluation, however, was performed with racemic α -fluoro samples.

In an attempt to optimize α -fluorination we explored several other possibilities, but a two-step enolization/ α -fluorination was the most successful. Interestingly, direct lithiation of ethoxy enone **5** with LDA⁴⁸ followed by α -fluorination with NFSI led to an inseparable mixture of 2- and 4-fluoro derivatives, and it was not further explored. On the other hand, enone **10**, which was accessed via the Sonogashira coupling reaction at 60 °C, was successfully enolized with LDA to give the TMS-enol ether in 60% conversion, but the reaction with NFSI failed to yield **11** under conditions analogous to those for the α -fluorination of **8** (Scheme 2). Similarly, under MacMillan's reaction conditions, product was not formed.

Next, α -fluoro enone **9** was reacted with methyl or ethyl hydroxylamine to afford the corresponding oximes **12** and **13** in a ratio of geometrical isomers *E*:*Z* of 1:2 (Scheme 2). These stable geometrical isomers were separable via column chromatography. The assignment of *E* and *Z* configuration of the oxime bond for isomers of **12** and **13** was initially made based on the ¹H NMR comparison to the known structure of **1** using the following principle. The hydrogen atom geminal to the fluorine atom (*H_f*, Figure 2a) is shifted downfield when closer through space to the oxime ether oxygen atom, and a hydrogen on the cyclohexenyl double bond (*H_{Cy}*) is shifted upfield when closer through space to the nitrogen atom lone pair and vice versa (Figure 2a). In a comprehensive study, Denmark and co-workers reported a similar geometrical assignment of oxime double bond based on strong anisotropic deshielding by the oxime oxygen on the equatorial protons at C₂ or C₆ positions.⁵⁵ Preference for the *Z*-isomer in this case was attributed to additional anomeric stabilization of the sp²

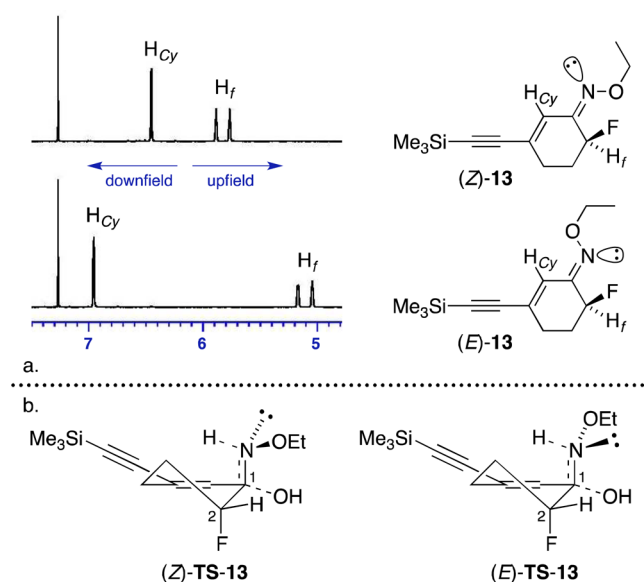
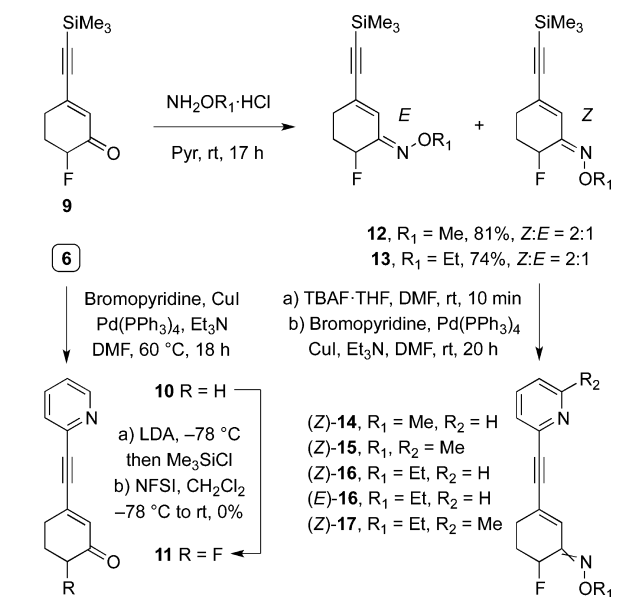
Scheme 2. Sonogashira Cross-Coupling Reaction To Form α -Fluoro Derivatives of [^{11}C]-1


Figure 2. (a) ^1H NMR analysis of *E*- and *Z*-isomers of **13**. (b) The anomeric stabilization rationale for a transition state (TS) leading to *Z*-isomer.

lone pair on the nitrogen by the σ^* bond between carbon atoms at C_1 and C_2 positions in (*Z*)-TS-13 (Figure 2b).

With oximes **12** and **13** in hand, deprotection of TMS-acetylene with TBAF was followed by the Sonogashira coupling to give rise to α -fluoro derivatives **14** to **17** in good yields (Table 1).

Crystallization of (*Z*)-**17** from Et₂O allowed for X-ray crystal structure analysis and confirmed the tentative configurational assignment of the oxime ether double bond. Notably, (*Z*)-**17** formed conglomerates, which could potentially be collected via triage to obtain each enantiomer (Figure 3).^{56–58} X-ray crystal

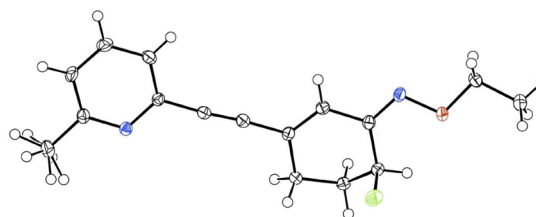


Figure 3. ORTEP diagram for (*Z*)-**17** showing *Z*-configuration of the ethyl oxime ether double bond. Fifty percent probability ellipsoids are plotted for non-hydrogen atoms.

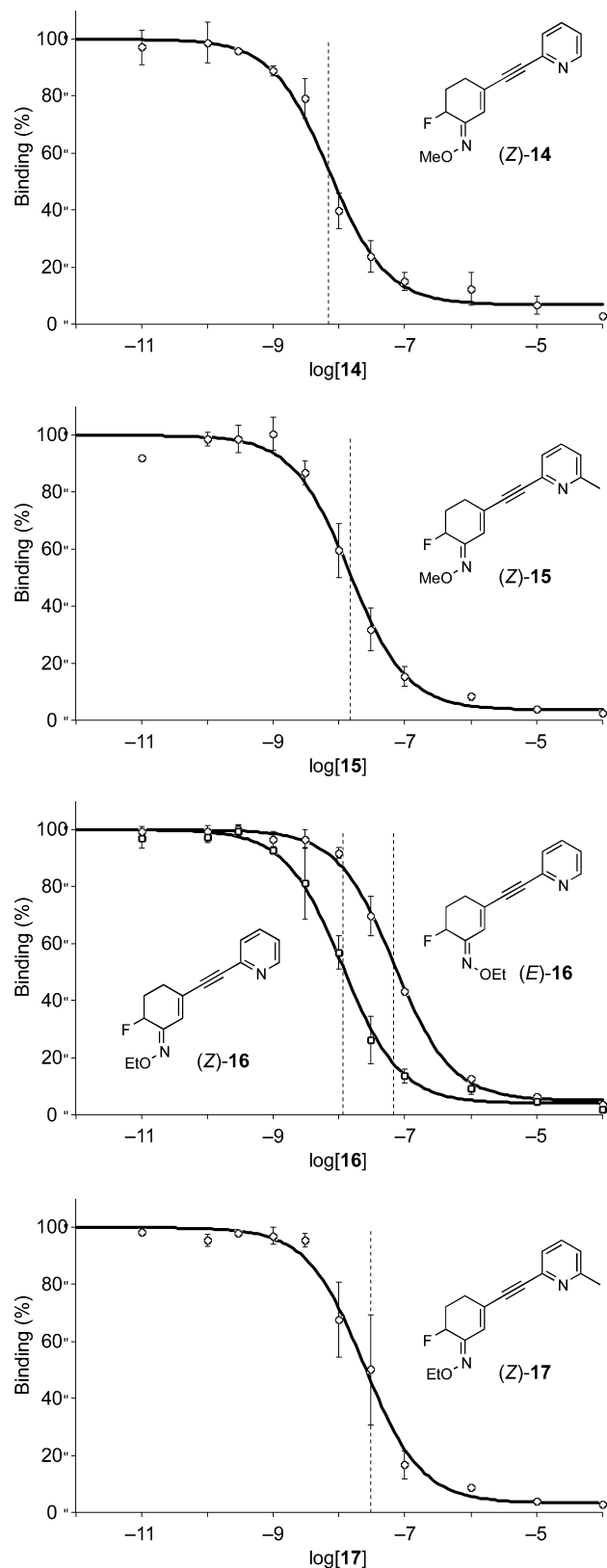
structure analysis revealed a preferred conformation with the fluorine atom in (*Z*)-**17** in the axial position, as anticipated from the geminal and vicinal coupling constants for H_f proton (47.3 and 2.6 Hz, respectively). This finding is in agreement with empirical observation made by the Stothers group for conformationally constrained α -fluoro cyclohexanones.⁵⁹

The biological evaluation of five derivatives **14**–**17** involved the binding affinity (K_i) determination (Table 1). For this purpose, a displacement assay with rat brain membranes was employed, and the IC_{50} displacement curves for all five derivatives are depicted in Chart 1. Structurally, the most similar analogue to **1** is methyl oxime ether (*Z*)-**15**, which showed reduced binding affinity in comparison to other investigated oxime ethers. Out of the five analogues, the two with the lowest K_i values, (*Z*)-**14** and (*Z*)-**16**, were further analyzed. Methyl oxime ether (*Z*)-**14** exhibited the highest binding affinity (3.4 nM), but the clogP and $\text{logD}_{7.4}$ values revealed low lipophilicity (1.7) of (*Z*)-**14**, which is below the optimal range for a brain mGluR5 PET tracer.⁴⁰ (Lipophilicity values provided in Table 1 were used solely as guidelines to establish relative relationship among investigated derivatives. Predicted (clogP) using in silico method and experimentally estimated ($\text{log D}_{7.4}$) using HPLC method values showed

Table 1. Product Yields of Sonogashira Cross-Coupling Reaction, Calculated (clogP), and Experimentally Estimated ($\text{log D}_{7.4}$) Lipophilicity Values and Related K_i Values As Determined via the Displacement Assay with [^3H]-**1**^a

entry	code	R_1	R_2	oxime geometry	coupling yield (%)	estimated		K_i (nM)
						clogP	$\text{log D}_{7.4}$	
1	14	Me	H	<i>Z</i>	63	1.7	1.7	3.4 ± 0.7
2	15	Me	Me	<i>Z</i>	68	2.2	2.0	8.5 ± 1.4
3	16	Et	H	<i>Z</i>	46	2.3	2.1	5.7 ± 2.2
4	16	Et	H	<i>E</i>	37	2.3	2.1/3.5 ^b	31.2 ± 2.4
5	17	Et	Me	<i>Z</i>	61	2.8	2.5	13.0 ± 6.7
6	1	Me	Me	<i>E</i>	–	2.4	2.3	4.4 ⁴⁰
7	1	Me	Me	<i>Z</i>	–	2.4	1.9	– ⁹

^a K_i values are estimated from measured IC_{50} values using the Cheng–Prusoff equation (see Supporting information). ^bValue calculated using the HPLC method/value determined using the shake flask method. Note: Entries 6 and 7 are nonfluorinated analogues.

Chart 1. [³H]-1 Displacement Curves for Derivatives 14–17^a

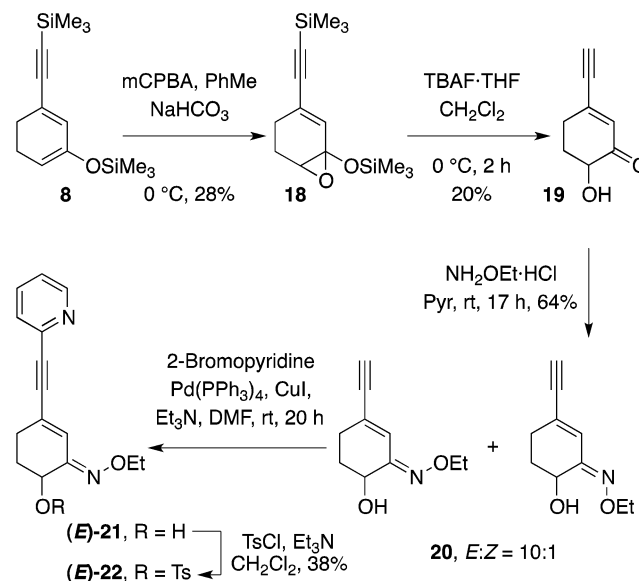
^aFor each compound, three experiments were performed in triplicate, and the average values are depicted in the curves (solid lines) fitted for one binding site. Dotted lines represent estimated IC_{50} values.

excellent agreement.) We therefore decided to evaluate ethyl oxime ether (*Z*)-16 which not only had a desired K_i value of 5.7 nM but also had a $clogP$ of 2.3. Interestingly, this SAR study revealed that the most significant difference in K_i was induced by the configuration of the oxime ether double bond (*E*- vs *Z*-16), similar to ABP688 oxime ether double bond isomers,⁹ and minimal change in K_i binding affinity is observed with variation of either the oxime ether (R_1 , Figure 1) or the pyridine ring (R_2 , Figure 1) functionalities.

It was then desired to introduce fluorine-18 into the molecule, but the application of an α -fluorination method using [¹⁸F]-NFSI⁶⁰ required an electrophilic source of fluorine-18 (¹⁸F₂), and this was not feasible for technical reasons. This was due to the nucleophilic nature (¹⁸F⁻) of the fluorine-18 source produced in the cyclotron in our facilities. An alternative approach was employed based on a nucleophilic substitution at the α -position to the oxime ether, which required the introduction of a suitable leaving group.

The tosyl leaving group was selected and the synthesis of radiolabeling precursor 22 (Scheme 3) was envisioned via a Rubottom oxidation^{61–63} of the previously prepared TMS-enol ether 8.

Scheme 3. Synthesis of Radiolabeling Precursor Tosylate (*E*)-22 via the Rubottom Oxidation



Trimethylsilyl enol ether 8 was treated with mCPBA⁶⁴ to afford epoxy enone 18 (Scheme 3). Enone 18 was purified only to remove mCPBA residue on a silica plug, and as such it was used for the next step in which the epoxide was opened under basic conditions using a TBAF·THF complex to give rise to α -hydroxy enone 19 in modest yields. α -Hydroxy enone 19 was further converted to ethyl oxime ether 20 by reaction with *O*-ethylhydroxylamine in 64% yield. To our surprise, the *Z*:*E* ratio of the oxime ether double bond was 1:10. Tentative assignment of oxime ether double bond geometry was made based on the γ -effect in the ¹³C NMR spectra^{65,66} of the two isomers (Figure 4a). In the two alkene molecules with all other identical components, the sterically compressed carbon atom at the allylic position is shifted upfield in comparison to the same carbon with a higher degree of steric freedom. We applied the γ -effect to ethyl oxime ethers (*Z*)-13 and (*E*)-13 to observe the

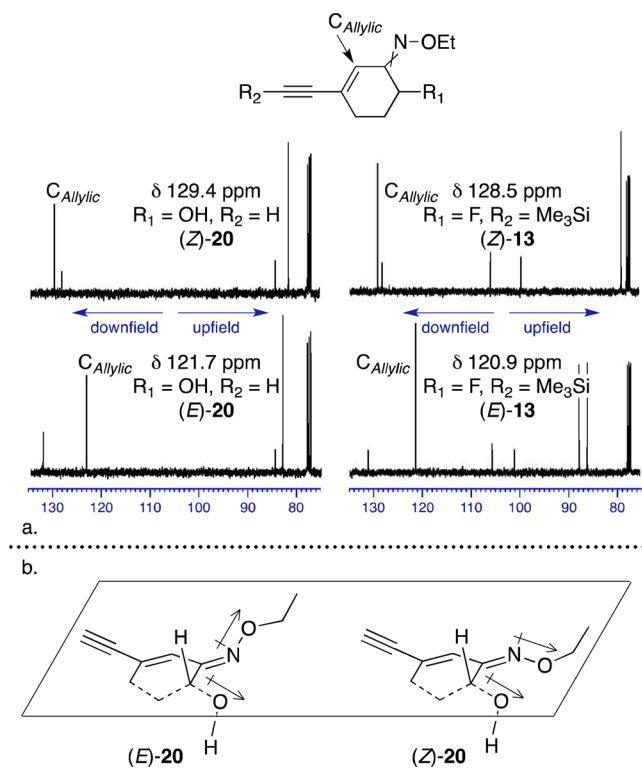


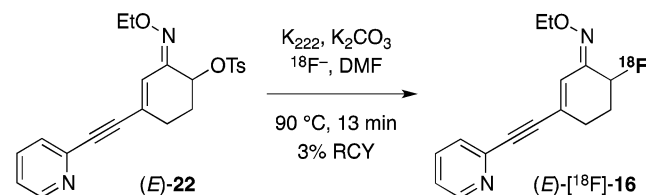
Figure 4. (a) Application of γ -effect for assignment of oxime ether double bond. (b) Dipole–dipole minimization rationale for the preference of *E*-isomer for α -hydroxy derivatives.

chemical shift of 7.6 ppm upfield for sterically compressed carbon atom $\text{C}_{\text{Allylic}}$ in (E)-13. A similar chemical shift of 7.7 ppm units upfield was found for α -hydroxy ethyl oxime ether (E)-20 for the $\text{C}_{\text{Allylic}}$ carbon atom with a lower degree of steric freedom (Figure 4a). Further confirmation of stereochemical assignment was sought, and the NOESY experiments performed for both geometrical isomers failed to detect NOE between $\text{C}_{\text{Allylic}}$ and the ethyl group from the oxime functionality presumably due to significant distance between the two. However, ^1H NMR showed comparable shifts as those seen in the fluorine case (Figure 2a). One possible explanation for the preference of the *E*-isomer could be postulated by invoking dipole–dipole interactions in **20** (Figure 4b). The *E*-isomer configuration facilitates minimization of dipole–dipole interactions.

At this juncture, we encountered another challenge of separating the two isomers. While the *E*-isomer was easily obtained in meaningful amounts, only trace amounts of *Z*-isomer were isolated after the purification, and we therefore selected the *E*-isomer of **16** for completion of the synthesis. Ethyl oxime ether (E)-20 was coupled with 2-bromopyridine under the Sonogashira reaction conditions to yield the alcohol (E)-21, which was tosylated to afford (E)-22 in 38% yield (Scheme 3). Both the Sonogashira cross-coupling and tosylation were performed under basic conditions, but no isomerization of the oxime ether double bond was observed. This finding was further compounded when tosylate (E)-22 was heated in deuterated chloroform over 3 h at 60 °C to show the full stability of the *E*-isomer.

We next investigated the radiolabeling of the model tosylate precursor (E)-22 in DMF using Kryptofix/ $^{18}\text{F}^-$ complex (Scheme 4). The radiolabeling was successful, albeit in low

Scheme 4. Radiolabeling of Precursor Tosylate (E)-22 To Afford (E)-[^{18}F]-16 in 3% Decay-Corrected Radiochemical Yield and 99% Purity As Determined by HPLC



radiochemical yield after purification via semipreparative HPLC to afford model radiotracer (E)-[^{18}F]-16 with 99% radiochemical purity. Initially performed at 90 °C for 10 min, a decay-corrected radiochemical yield of 2% was obtained. A slight improvement to 3% was accomplished by increasing the reaction time to 13 min. The identity of the product was confirmed through coinjection with cold reference (E)-16; however, under the employed HPLC conditions for quality control, *E*- and *Z*-isomers were inseparable. Due to similar polarity of the two isomers, only partial separation was accomplished using LiChrosorb column to show an *E*:*Z* ratio of ca. 9:1, suggesting partial isomerization of the oxime ether double bond during radiolabeling. A similar observation was made for [^{11}C]-ABP688 where typical *E*:*Z* ratio was ca. 10:1.⁹

The stability of the model compound (E)-[^{18}F]-16 was determined, and over a period of 2 h, PET radiotracer (E)-[^{18}F]-16 was stable when incubated at 37 °C in both rat plasma and PBS. (*Z*)-Derivatives **14** to **17** are likely to exhibit similar stability in plasma and PBS.

Lipophilicity of (E)-[^{18}F]-16 was determined using a shake flask method to show $\log D_{7.4}$ of 3.5 ± 0.1 , significantly higher than that predicted by the *in silico* method (2.3), or experimentally estimated using HPLC method (2.1).

The equilibrium dissociation constant K_d of (E)-[^{18}F]-16 was further explored in a Scatchard assay (see Supporting Information). A K_d value of 70 nM was estimated for (E)-[^{18}F]-16 in a single experiment performed in triplicate which was in complete agreement with the previously determined IC_{50} (68 nM).

Radiolabeled (E)-[^{18}F]-16 also served as a model compound to establish if the binding was specific to mGluR5 *in vitro*. The autoradiographic study was performed on rat brain slices using 1 or 10 nM solutions of (E)-[^{18}F]-16 (Figure 5). Importantly, the distribution of radioactivity was heterogeneous, and the highest uptake was observed in regions where mGluR5 is highly expressed in the brain (i.e., hippocampus and cortex).

Additionally, the brain slices were incubated with the solution of (E)-[^{18}F]-16 (1 or 10 nM) and cold **1** (100 nM). A complete blockade of radioactivity was observed, indicating that (E)-[^{18}F]-16 specifically binds to mGluR5 *in vitro* (Figure 5).

CONCLUSIONS

In the search for a fluorine-18-labeled PET radiotracer for imaging mGluR5, we have successfully synthesized and structurally assigned five novel derivatives based on the structural manifold of [^{11}C]-1 by employing an enolization/NFSI α -fluorination method. Our *in vitro* data enabled identification of (Z)-16 as a potential mGluR5 PET radiotracer. However, the synthesis of the tosylate precursor **22** revealed a stereochemical preference for the *E*-isomer of α -hydroxy derivative (E)-20 which prompted us to prepare (E)-[^{18}F]-16

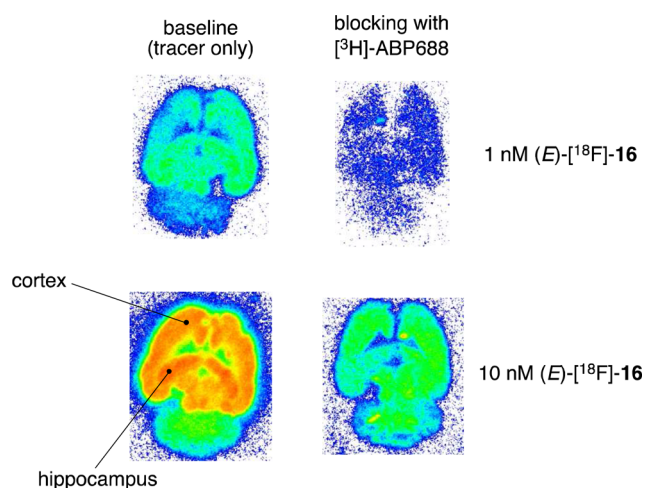


Figure 5. Autoradiography on horizontal rat brain slices, indicating heterogeneous distribution of activity with highest uptake in mGluR5-rich regions. The first and second rows represent application of 1 and 10 nM ^{18}F -16, respectively, and the first and second column represent baseline and blocking conditions, respectively.

as a model compound for the establishment of a radiolabeling strategy and in vitro testing. We successfully radiosynthesized (E) - ^{18}F -16 and demonstrated its stability in vitro in plasma and PBS and specificity to mGluR5. Encouraged by the success of fluorine-18 radiolabeling in an α -position of the oxime ether double bond and the heterogeneous mGluR5 specific uptake of (E) - ^{18}F -16 in rat brain slices in vitro, exploration of alternative routes to access the *Z*-isomer selectively are currently underway in our lab. The results of these studies will be reported in due course.

MATERIALS AND METHODS

General Techniques. All reactions requiring anhydrous conditions were conducted in flame-dried glass apparatus under an atmosphere of inert gas. All chemicals and anhydrous solvents were purchased from Aldrich or ABCR and used as received unless otherwise noted. Reported density values are for ambient temperature. ^3H -1 (2.405 GBq/ μmol , 37 MBq/mL solution in EtOH) was obtained from AstraZeneca. Purity of compounds was $\geq 95\%$ as determined by analytical HPLC method on an Agilent HPLC system. Preparative chromatographic separations were performed on Aldrich Science silica gel 60 (35–75 μm) and reactions followed by TLC analysis using Sigma-Aldrich silica gel 60 plates (2–25 μm) with fluorescent indicator (254 nm) and visualized with UV or potassium permanganate. Infrared spectra were recorded on a JASCO FT/IR 6200 (OmniLab) spectrometer using a chloroform solution of compound. ^1H and ^{13}C NMR spectra were recorded in Fourier transform mode at the field strength specified on Bruker Avance FT-NMR spectrometers. Spectra were obtained from the specified deuterated solvents in 5 mm diameter tubes. Chemical shift in ppm is quoted relative to residual solvent signals calibrated as follows: CDCl_3 δ_{H} (CHCl_3) = 7.26 ppm, δ_{C} = 77.2 ppm; $(\text{CD}_3)_2\text{SO}$ δ_{H} ($\text{CD}_3\text{SOCHD}_2$) = 2.50 ppm, δ_{C} = 39.5 ppm. Multiplicities in the ^1H NMR spectra are described as follows: s = singlet, d = doublet, t = triplet, q = quartet, quint. = quintet, m = multiplet, b = broad; coupling constants are reported in hertz. Numbers in parentheses following carbon atom chemical shifts refer to the number of attached hydrogen atoms as revealed by the DEPT spectral editing technique. Electrospray (ES) mass spectra (LRMS) were obtained with a Micromass Quattro micro API LC electrospray ionization, and electrospray (ES) mass spectra (HRMS) were obtained with a Bruker FTMS 4.7 T BioAPEXII spectrometer. Electron-impact (EI) and chemical ionization (CI) mass spectra (LRMS and HRMS) were

obtained with a Waters Micromass AutoSpec Ultima MassLynx 4.0 spectrometer. Ion mass/charge (m/z) ratios are reported as values in atomic mass units. Semipreparative purification of radiolabeled material was performed on a Merck-Hitachi L6200A system equipped with Knauer variable wavelength detector and an Eberline radiation detector using a reverse phase column (C18 Phenomenex Gemini, 5 μm , 250 \times 10 mm) and eluting with the following gradient: 0–5 min 5% aq MeCN, 5–15 min 5–50% aq MeCN, 15–30 min 50% aq MeCN, 30–50 min, 50–90% aq MeCN, 50–65 min, 65% MeCN at flow rate 5 mL/min. Analytical HPLC samples were analyzed by an Agilent HPLC 1100 system equipped with a UV multiwavelength detector and a Raytest Gabi star radiation detector using a reverse phase column (ACE 111-0546, C18, 3 μm , 50 \times 4.6 mm) and eluting with 45% aq MeCN at flow rate 1 mL/min. Samples for PBS and plasma stability were analyzed by HPLC using an Agilent 1100 system with Gina software, equipped with UV multiwavelength and Raytest Gabi Star detectors. For HPLC analysis, a reversed phase column (Phenomenex, Gemini 10 μm C18 column, 300 \times 3.9 mm, Phenomenex) was used at 1 mL/min flow of 70% aq MeCN.

Trimethyl((5-((trimethylsilyl)ethynyl)cyclohexa-1,5-dien-1-yl)oxy)silane (8). A one-neck round-bottom flame-dried flask was charged at ambient temperature under N_2 atmosphere with anhydrous tetrahydrofuran (8 mL), diisopropylamine (0.77 mL, 554 mg, 5.49 mmol, $d = 0.722$) was added, and the colorless solution was cooled to -20°C (few pieces of dry ice in the acetone bath). The mixture was then treated with *n*-butyllithium (3.5 mL, 4.99 mmol, $c = 1.43$ M solution in hexanes) dropwise via syringe over 2 min, and the resulting pale yellow solution was stirred for 36 min. After this time, the pale yellow clear LDA solution was further cooled to -78°C (dry ice/acetone bath), and it was then treated with a solution of 3-ethynylcyclohex-2-enone (500 mg, 4.16 mmol) in anhydrous tetrahydrofuran (4 mL) dropwise via syringe over 9 min during at which time the mixture turned brown (on the surface purple coloration was observed) and a precipitate formed. The resulting heterogeneous mixture was stirred at -78°C under N_2 atmosphere for 64 min. After this time, chlorotrimethylsilane (1.0 mL, 904 mg, 8.32 mmol, $d = 0.856$) was added in one portion, and the resulting mixture was stirred at -78°C under N_2 for 64 min, during which time the mixture turned bright orange and clear. After this time, the cooling bath was removed, the orange clear mixture was allowed to warm to ambient temperature over 30 min, and the crude mixture was then poured over ice-cold 5% wt aq NaHCO_3 (40 mL) and was diluted with Et_2O (50 mL). The two layers were shaken well and separated. The organic phase was washed with H_2O (3 \times 35 mL) and brine (1 \times 35 mL), dried (Na_2SO_4), and concentrated in vacuo to give crude material as a bright red oily residue (1.0 g, 3.79 mmol, 91%). The crude mixture was used for the next step without further purification: ^1H NMR (400 MHz, CDCl_3) δ 6.06 (bd, $J = 1.8$ Hz, 1H), 5.02–4.96 (m, 1H), 2.24–2.20 (m, 4H), 0.20 (s, 9H), 0.19 (s, 9H) ppm.

6-Fluoro-3-((trimethylsilyl)ethynyl)cyclohex-2-enone (9). At ambient temperature under N_2 atmosphere, a one-neck round-bottom flask was charged with the crude mixture of trimethyl((5-((trimethylsilyl)ethynyl)cyclohexa-1,5-dien-1-yl)oxy)silane (1.08 g, 4.10 mmol), anhydrous dichloromethane (6 mL) was added, and the resulting clear red mixture was cooled to -78°C (dry ice/acetone bath). The mixture was then treated with *N*-fluorodibenzene sulfonamide (1.30 g, 4.10 mmol, 97% pure) portionwise (with each portion, the flask was quickly opened to air) over 4 min, and the resulting brown heterogeneous mixture was stirred under N_2 and slowly warmed to ambient temperature over 26.5 h. After this time, the crude reaction mixture was quenched with 0.1 M aq HCl (7 mL), the mixture was further diluted with H_2O (7 mL) and CH_2Cl_2 (12 mL), and the two layers were shaken well and separated. The aqueous phase was extracted with CH_2Cl_2 (2 \times 12 mL). The combined organic extracts were dried (Na_2SO_4) and concentrated in vacuo to give crude material as a red oily residue (2.56 g) which was purified by chromatography on a silica gel column (eluting with 5% EtOAc/pentane) to give the title compound (205 mg, 0.97 mmol, 24%) as a pale yellow oil: IR (neat) 2962, 2904, 1696, 1591, 1430, 1354, 1253, 1203, 1154, 1096, 846, 765, 703 cm^{-1} ; ^1H NMR (400 MHz, CDCl_3) δ

6.24–6.22 (m, 1H), 4.91 (ddd, $J = 48.0, 12.2, 5.1$ Hz, 1H), 2.67–2.60 (m, 2H), 2.47–2.16 (m, 2H), 0.23 (s, 9H) ppm; ^{13}C NMR (100 MHz, CDCl_3) δ 193.3 (d, $J = 15.3$ Hz, 0), 143.4 (0), 131.4 (1), 108.2 (0), 102.6 (0), 89.7 (d, $J = 186$ Hz, 1), 29.4 (d, $J = 12.6$ Hz, 2), 29.3 (d, $J = 3.6$ Hz, 2), -0.31 (3) ppm; ^{19}F NMR (376 MHz, CDCl_3) δ -192.4 (dm, $J = 49.3$ Hz) ppm; MS (ES+) m/z 211 ($M + H$) $^+$; HRMS (ESI) m/z 211.0938 (calcd for $\text{C}_{11}\text{H}_{16}\text{FOSi}$: 211.0949).

6-Fluoro-3-((trimethylsilyl)ethynyl)cyclohex-2-enone O-Ethyl Oxime (13). At ambient temperature under an Ar atmosphere, a pear-shaped flask was charged with 6-fluoro-3-((trimethylsilyl)ethynyl)cyclohex-2-enone (150 mg, 0.71 mmol), pyridine (2.4 mL) was added, and the resulting pale clear mixture was further treated with *O*-ethylhydroxylamine hydrochloride (104 mg, 1.07 mmol) in one portion. The resulting mixture was stirred at ambient temperature under Ar for 21 h. After this time, the mixture was diluted with H_2O (6 mL) and Et_2O (10 mL), and the two layers were shaken well and separated. The aqueous phase was extracted with Et_2O (2×10 mL). The combined organic extracts were washed with saturated aq CuSO_4 (3×7 mL), H_2O (1×10 mL), and brine (1×10 mL), dried (Na_2SO_4), and concentrated in vacuo to give crude material as a pale brown oil. The crude mixture was purified by chromatography on a silica gel column (eluting with 2% EtOAc/pentane) to give (*Z*)-6-fluoro-3-((trimethylsilyl)ethynyl)cyclohex-2-enone *O*-ethyl oxime (86.7 mg, 0.34 mmol, 48%): IR (neat) 2958, 2146, 1360, 1250, 1051, 987, 843, 760 cm^{-1} ; ^1H NMR (400 MHz, CDCl_3) δ 6.46 (dm, $J = 2.8$ Hz, 1H), 5.83 (dt, $J = 47.5, 2.8$ Hz, 1H), 4.22 (ddm, $J = 7.1, 6.0$ Hz, 2H), 2.61–2.59 (m, 1H), 2.33–2.20 (m, 2H), 1.73 (dm, $J = 46.4$ Hz, 1H), 1.30 (t, $J = 7.1$ Hz, 3H), 0.21 (s, 9H) ppm; ^{13}C NMR (100 MHz, CDCl_3) δ 150.7 (d, $J = 13.7$ Hz, 0), 128.5 (d, $J = 1.2$ Hz, 1), 127.6 (d, $J = 2.3$ Hz, 0), 105.4 (0), 99.1 (0), 77.8 (d, $J = 167$ Hz, 1), 70.8 (2), 27.7 (d, $J = 22.3$ Hz, 2), 24.6 (d, $J = 3.2$ Hz, 2), 14.7 (3), 0.0 (3) ppm; ^{19}F NMR (376 MHz, CDCl_3) δ -188.5 (td, $J = 47.0, 12.4$ Hz) ppm; MS (ES+) m/z 254 ($M + H$) $^+$; HRMS (ESI) m/z 254.1373 (calcd for $\text{C}_{13}\text{H}_{21}\text{FNOSi}$: 254.1371) and (*E*)-6-fluoro-3-((trimethylsilyl)ethynyl)cyclohex-2-enone *O*-ethyl oxime (46.8 mg, 0.18 mmol, 26%): IR (neat) 2960, 2142, 1595, 1573, 1428, 1250, 1049, 975, 842, 760, 638 cm^{-1} ; ^1H NMR (400 MHz, CDCl_3) δ 6.96 (dm, $J = 2.7$ Hz, 1H), 5.11 (dm, $J = 49.2$ Hz, 1H), 4.21 (q, 7.0 Hz, 2H), 2.66–2.53 (m, 1H), 2.39–2.28 (m, 2H), 1.85 (dm, $J = 43.2$ Hz, 1H), 1.30 (t, $J = 7.1$ Hz, 3H), 0.22 (s, 9H) ppm; ^{13}C NMR (100 MHz, CDCl_3) δ 148.5 (d, $J = 16.7$ Hz, 0), 130.6 (d, $J = 2.8$ Hz, 0), 120.9 (1), 105.2 (0), 100.7 (0), 86.6 (d, $J = 169$ Hz, 1), 70.6 (2), 28.3 (d, $J = 22.8$ Hz, 2), 25.8 (d, $J = 4.8$ Hz, 2), 14.7 (3), 0.0 (3) ppm; ^{19}F NMR (376 MHz, CDCl_3) δ -178.5 (ddd, $J = 50.4, 43.2, 7.9$ Hz) ppm; MS (ES+) m/z 254 ($M + H$) $^+$; HRMS (ESI) m/z 254.1375 (calcd for $\text{C}_{13}\text{H}_{21}\text{FNOSi}$: 254.1371).

(Z)-6-Fluoro-3-(pyridin-2-ylethynyl)cyclohex-2-enone O-Ethyl Oxime ((Z)-16). At ambient temperature under a N_2 atmosphere, a one-neck pear-shaped flask was charged with (*Z*)-6-fluoro-3-((trimethylsilyl)ethynyl)cyclohex-2-enone *O*-ethyl oxime (43 mg, 0.17 mmol), anhydrous N,N -dimethylformamide (0.8 mL) was added, and the resulting pale yellow solution was further treated with tetrabutylammonium fluoride solution in tetrahydrofuran (0.34 mL, 0.34 mmol, $c = 1$ M) dropwise over 1 min during which time the mixture turned brown. Then the mixture was stirred for 13 min. TLC analysis indicated that all starting material was consumed, and without workup and/or further purification, the mixture was used for the next step. A two-neck round-bottom flask was evacuated at ambient temperature, and it was then backfilled with N_2 , repeating this three times. This flask was then charged with the crude reaction mixture of (*Z*)-3-ethynyl-6-fluorocyclohex-2-enone *O*-ethyl oxime (31 mg, 0.17 mmol, still containing TBAF·THF and DMF), and additional anhydrous N,N -dimethylformamide (1.5 mL) was used for quantitative transfer. The resulting red mixture was further treated with 2-bromopyridine (16 μL , 27.0 mg, 0.17 mmol, $d = 1.657$) followed by triethylamine (0.28 mL, 206 mg, 2.04 mmol, $d = 0.726$), and then copper(I) iodide (3.2 mg, 17.0 μmol) was added in one portion (flask was quickly opened to the air). Finally tetrakis(triphenylphosphine)-palladium(0) (6.0 mg, 5.1 μmol) was added in one portion (the flask was once again opened to air quickly), and the resulting brown

mixture was stirred at ambient temperature for 22 h. After this time, the brown mixture was quenched with saturated aq NH_4Cl (8 mL) and then diluted with H_2O (3 mL) and EtOAc (11 mL), and the two layers were shaken well and separated. The aqueous phase was extracted with EtOAc (2×11 mL). The combined organic phase was washed with H_2O (3×8 mL) and brine (1×8 mL), dried (Na_2SO_4), and concentrated in vacuo to give crude material as a brown oily residue (338 mg) which was then purified by chromatography on a silica gel column (eluting with gradient 20–30% EtOAc/pentane) to give the title compound (20 mg, 0.08 mmol, 46%) as a pale yellow oil: IR (neat) 2978, 2933, 1580, 1562, 1462, 1428, 1048, 987, 959, 891, 859, 779 cm^{-1} ; ^1H NMR (400 MHz, CDCl_3) δ 8.60 (ddd, $J = 4.9, 1.7, 1.0$ Hz, 1H), 7.66 (td, $J = 7.7, 1.8$ Hz, 1H), 7.45 (dt, $J = 7.8, 1.1$ Hz, 1H), 7.23 (ddd, $J = 7.6, 4.9, 1.2$ Hz, 1H), 6.59 (dm, $J = 2.6$ Hz, 1H), 5.86 (dt, $J = 47.4, 2.5$ Hz, 1H), 4.24 (ddm, $J = 7.1, 5.8$ Hz, 2H), 2.71–2.59 (m, 1H), 2.43–2.26 (m, 2H), 1.79 (dm, $J = 46.3$ Hz, 1H), 1.31 (t, $J = 7.0$ Hz, 3H) ppm; ^{13}C NMR (100 MHz, CDCl_3) δ 150.4 (d, $J = 13.7$ Hz, 0), 150.1 (1), 143.1 (0), 136.1 (1), 129.0 (d, $J = 1.1$ Hz, 1), 127.3 (1), 126.6 (d, $J = 2.2$ Hz, 0), 123.1 (d, $J = 20.0$ Hz, 1), 92.4 (0), 89.3 (0), 77.6 (d, $J = 167$ Hz, 1), 70.8 (3), 27.5 (d, $J = 22.2$ Hz, 1), 24.3 (d, $J = 3.2$ Hz, 1), 14.5 (3) ppm; ^{19}F NMR (376 MHz, CDCl_3) δ -188.4 (td, $J = 47.0, 12.0$ Hz) ppm; MS (ES+) m/z 259 ($M + H$) $^+$; HRMS (ESI) m/z 259.1240 (calcd for $\text{C}_{15}\text{H}_{16}\text{FN}_2\text{O}$: 259.1241).

(E)-6-Fluoro-3-(pyridin-2-ylethynyl)cyclohex-2-enone O-Ethyl Oxime ((E)-16). A method analogous to that described for (*Z*)-16 was employed, starting with (*E*)-6-fluoro-3-((trimethylsilyl)ethynyl)cyclohex-2-enone *O*-ethyl oxime (48 mg, 0.19 mmol) to give crude material as a brown oily residue which was then purified by chromatography on a silica gel column (eluting with 20% EtOAc/pentane) to give the title compound (18 mg, 0.07 mmol, 37%) as a pale yellow oil: IR (neat) 2977, 2934, 1581, 1463, 1429, 1369, 1049, 977, 912, 890, 781, 742 cm^{-1} ; ^1H NMR (400 MHz, CDCl_3) δ 8.62 (ddd, $J = 4.8, 1.7, 0.9$ Hz, 1H), 7.68 (td, $J = 7.7, 1.8$ Hz, 1H), 7.47 (dt, $J = 7.8, 1.1$ Hz, 1H), 7.25 (ddd, $J = 7.6, 4.9, 1.2$ Hz, 1H), 7.14 (dm, $J = 2.7$ Hz, 1H), 5.15 (dm, $J = 50.1$ Hz, 1H), 4.23 (qd, $J = 7.1, 0.6$ Hz, 2H), 2.77–2.64 (m, 1H), 2.51–2.33 (m, 2H), 1.91 (dm, $J = 43.3$ Hz, 1H), 1.31 (t, $J = 7.1$ Hz, 3H) ppm; ^{13}C NMR (100 MHz, CDCl_3) δ 150.4 (1), 148.3 (d, $J = 16.6$ Hz, 0), 143.0 (0), 136.4 (1), 129.8 (0), 127.6 (1), 123.4 (1), 121.8 (1), 93.6 (0), 89.3 (0), 86.5 (d, $J = 170$ Hz, 1), 70.7 (2), 28.4 (d, $J = 22.6$ Hz, 2), 25.5 (d, $J = 4.7$ Hz, 2), 14.6 (3) ppm; ^{19}F NMR (376 MHz, CDCl_3) δ -178.4 (ddd, $J = 50.7, 43.2, 8.3$ Hz) ppm; MS (ES+) m/z 259 ($M + H$) $^+$; HRMS (ESI) m/z 259.1236 (calcd for $\text{C}_{15}\text{H}_{16}\text{FN}_2\text{O}$: 259.1241).

X-ray Analysis: Crystal Data for (Z)-17. $\text{C}_{16}\text{H}_{17}\text{FN}_2\text{O}$, $M_w = 272.32$, orthorhombic space group $P2_12_12_1$, $a = 6.2820(1)$ Å, $b = 11.4820(3)$ Å, $c = 19.6867(5)$ Å; data measurement performed on a Bruker APEX II Duo diffractometer at 100 K, radiation Mo $\text{K}\alpha$ ($\lambda = 0.71073$ Å), $z = 4$, $R = 0.032$ for $3090 I > 2\sigma(I)$, 0.033 for all 3248 unique reflections, GOF = 1.16. Full crystallographic data have been deposited with the Cambridge Crystallographic Data Centre under deposition number CCDC 880418 and can be obtained free of charge via www.ccdc.cam.ac.uk/.

(E)-6-Fluoro-3-(pyridin-2-ylethynyl)cyclohex-2-enone O-Ethyl Oxime ((E)- ^{18}F)-16. No-carrier-added [^{18}F]-fluoride was produced via nuclear $^{18}\text{O}(p, n)^{18}\text{F}$ reaction from enriched ^{18}O -water using an IBA cyclone 18/9 cyclotron, and it was immediately trapped on a QMA cartridge (preconditioned with 0.5 M aq K_2CO_3 (1×5 mL) and then H_2O (1×5 mL) and dried in air). The trapped [^{18}F]-fluoride was eluted from the cartridge with 0.25 wt % Kryptofix-222 solution (1 mL) in basic (0.05 wt % K_2CO_3) aq MeCN (75% v/v) into a tightly closed reaction vial. The solvents were evaporated in vacuo (130 mbar) with a gentle stream of N_2 gas at 110 °C over 5 min. To the resulting solid residue was then added anhydrous MeCN (1 mL), and the mixture was azeotropically dried in vacuo (130 mbar) with a gentle stream of N_2 at 110 °C. To the dried Kryptofix-222/[^{18}F] complex was added a solution of (*E*)-22 (2.19 mg, 5.33 μmol) in anhydrous N,N -dimethylformamide (0.3 mL), and the dark brown mixture was heated at 90 °C for 13 min. The crude mixture was diluted with 50% v/v aq MeCN (2 mL) and purified via semipreparative HPLC. The desired product was collected (retention

time: 30.9 min) and immediately diluted with H₂O (10 mL). The aqueous solution was passed through a C18 cartridge (preconditioned with EtOH (1 × 5 mL) and then H₂O (1 × 5 mL) and dried in air), the cartridge was washed with H₂O (2 × 1 mL), and the product was eluted from the C18 cartridge with EtOH (1 × 0.3 mL) into a sterile vial containing 50% aq PEG200 (5 mL) to afford the radiolabeled title compound in a 3% decay-corrected yield. Typically, starting from ca. 35 GBq of activity, 740 MBq of product was obtained. The radiochemical purity was >99%, and specific activity was 30 GBq/μmol.

Competition Binding Assay. Brain membranes were prepared from Sprague–Dawley rat brains as described previously.⁴⁰ Frozen membranes were thawed on ice and pelleted at 4500g at 4 °C for 5 min. The membranes were washed twice with HEPES buffer (30 mM HEPES, 110 mM NaCl, 5 mM KCl, 2.5 mM CaCl₂, 1.2 mM MgCl₂, pH 8 at 4 °C) and resuspended in HEPES buffer at a protein concentration of 1.3 mg/mL. The binding assay was performed as previously described.⁴⁰ In brief, brain membranes (0.1 mg of protein) were incubated in triplicate at ambient temperature with 2 nM [³H]-1 and (*E*)-16 at concentrations between 10 pM and 100 μM in a total volume of 0.2 mL of HEPES. (*E*)-16 was diluted from a 1 mM ethanolic (50%) solution. The corresponding EtOH concentrations did not affect [³H]-1 binding (data not shown). Nonpecific binding of [³H]-1 was estimated with 100 μM MMPEP. After 45 min, the samples were filtered, and the filters containing the membranes with bound [³H]-1 were measured in a β-counter (Beckman LS6500). Bound [³H]-1 (B, pmol per mg protein) was fitted with Excel solver to eq 1 to estimate IC₅₀.

$$B = B_{\min} + ((B_{\max} - B_{\min}) / (1 + (C / IC_{50}))) \quad (1)$$

where *C* is the total (*E*)-16 concentration, *B*_{max} is the maximal *B*, i.e., the plateau in the *B/C* plot at low log *C* and *B*_{min} is the minimal *B*, i.e., the plateau at high log *C*. The inhibition constant *K*_i of (*E*)-16 was estimated from the IC₅₀ and *K*_d of [¹¹C]-1 (1.7 ± 0.2 nM)⁹ with the Cheng–Prusoff equation.

Stability in PBS and Plasma. (*E*)-[¹⁸F]-16 (21 MBq) was incubated in phosphate buffer (4 mM KH₂PO₄/Na₂HPO₄, 155 mM NaCl, pH 7.4) or rat plasma at 37 °C for up to 2 h. At different time points, samples were^{61–63} diluted and reactions stopped with ice-cold MeCN (140 μL). Plasma samples were centrifuged at 12000g for 10 min. The samples were filtered, and supernatants were analyzed by HPLC.

In Vitro Autoradiography. Frozen horizontal brain slices (20 μm) from a male Wistar rat (221 g) adsorbed to SuperFrost Plus slides were thawed at ambient temperature and preincubated on ice for 10 min in HEPES buffer (see above) containing 0.1% bovine serum albumin (BSA). Excess solution was carefully removed, and slides were incubated with 1 or 10 nM (*E*)-[¹⁸F]-16 alone or together with 100 nM 1 in HEPES buffer for 45 min at ambient temperature. After incubation, the solutions were decanted and the slides washed on ice in HEPES buffer containing 0.1% BSA and twice in HEPES buffer (3 min each) and finally dipped in H₂O. Dried slides were exposed to a phosphor imager plate for 30 min, and the plate was scanned in a BAS5000 reader (Fuji).

■ ASSOCIATED CONTENT

Ⓢ Supporting Information

Full experimental procedures and characterization of all compounds, NMR data, HPLC and GC traces, IC₅₀ binding curves, Scatchard plot for (*E*)-[¹⁸F]-16, and original X-ray crystallography data for (*Z*)-17. This material is available free of charge via the Internet at <http://pubs.acs.org>.

■ AUTHOR INFORMATION

Corresponding Author

*Phone: +41 44 6337463. E-mail: simon.ametamey@pharma.ethz.ch.

Author Contributions

All authors have given approval to the final version of the manuscript.

Notes

The authors declare no competing financial interest.

■ ACKNOWLEDGMENTS

The authors acknowledge Mrs. Petra Wirth and Dr. Adrienne Müller for technical support. Professor Paul R. Blakemore (Oregon State University) is acknowledged for helpful discussions on NMR assignments. Drs. Bernhard Pfeiffer (Altman group) and Marc-Olivier Ebert (Laboratory for Organic Chemistry, ETH) are acknowledged for technical support with NMR analysis. Dr. Ebert is acknowledged for performing additional NOE experiments for compounds (*E*)-20 and (*Z*)-20. Ms. Sara Wyss (Werner group) is acknowledged for performing chiral GC analysis of *ent*-9. Dr. Mark A. Sephton (ZHAW) is acknowledged for proofreading the manuscript. Ms. Cindy Fisher, Drs. Cindy A. Wanger-Baumann, and Thomas Betzel are acknowledged for useful discussions.

■ ABBREVIATIONS USED

mGluR5, metabotropic glutamate receptor subtype 5; PET, positron emission tomography; NFSI, *N*-fluorodibenzene-sulfonamide; mCPBA, *m*-chloroperbenzoic acid; DMF, *N,N'*-dimethylformamide; THF, tetrahydrofuran; [¹¹C]-ABP688, (*E*)-3-((6-methylpyridin-2-yl)ethynyl)cyclohex-2-enone *O*-[¹¹C]methyl oxime; [³T]-ABP688, (*E*)-3-((6-methylpyridin-2-yl)ethynyl)cyclohex-2-enone *O*-[³T]methyl oxime; [¹⁸F]-SP203, 3-fluoro-5-(2-([¹⁸F](fluoromethyl)thiazol-4-yl)ethynyl)benzotrile; [¹⁸F]-FPEB, 3-[¹⁸F]fluoro-5-(2-pyridinylethynyl)benzotrile; [¹⁸F]-FDEGPECO, (*E*)-3-(pyridin-2-ylethynyl)cyclohex-2-enone *O*-(2-(2-[¹⁸F]uoroethoxy)ethyl) oxime; MMPEP, 2-[(3-methoxyphenyl)ethynyl]-6-methylpyridine; PBS, phosphate buffer in saline; SAR, structure–activity relationship; TLC, thin layer chromatography; HPLC, high pressure liquid chromatography; GC, gas chromatography; IC₅₀, half maximal inhibitory concentration; *K*_i, inhibition constant; *K*_d, dissociation constant

■ REFERENCES

- (1) Ametamey, S. M.; Honer, M.; Schubiger, P. A. *Chem. Rev.* **2008**, *108*, 1501.
- (2) Jacobs, A. H.; Li, H.; Winkler, A.; Hilker, R.; Knoess, C.; Ruger, A.; Galldiks, N.; Schaller, B.; Sobesky, J.; Kracht, L.; Monfared, P.; Klein, M.; Vollmar, S.; Bauer, B.; Wagner, R.; Graf, R.; Wienhard, K.; Herholz, K.; Heiss, W. D. *Eur. J. Nucl. Med. Mol. Imaging* **2003**, *30*, 1051.
- (3) Mu, L.; Schubiger, P. A.; Ametamey, S. M. *Curr. Top. Med. Chem.* **2010**, *10*, 1558.
- (4) Pin, J. P.; Duvoisin, R. *Neuropharmacology* **1995**, *34*, 1.
- (5) Shigemoto, R.; Kinoshita, A.; Wada, E.; Nomura, S.; Ohishi, H.; Takada, M.; Flor, P. J.; Neki, A.; Abe, T.; Nakanishi, S.; Mizuno, N. *J. Neurosci.* **1997**, *17*, 7503.
- (6) Shigemoto, R.; Mizuno, N. *Handb. Chem. Neuroanat.* **2000**, *18*, 63.
- (7) Shigemoto, R.; Nomura, S.; Ohishi, H.; Sugihara, H.; Nakanishi, S.; Mizuno, N. *Neurosci. Lett.* **1993**, *163*, 53.
- (8) Tanabe, Y.; Masu, M.; Ishii, T.; Shigemoto, R.; Nakanishi, S. *Neuron* **1992**, *8*, 169.
- (9) Ametamey, S. M.; Kessler, L. J.; Honer, M.; Wyss, M. T.; Buck, A.; Hintermann, S.; Auberson, Y. P.; Gasparini, F.; Schubiger, P. A. *J. Nucl. Med.* **2006**, *47*, 698.

- (10) Ametamey, S. M.; Treyer, V.; Streffer, J.; Wyss, M. T.; Schmidt, M.; Blagoev, M.; Hintermann, S.; Auberson, Y.; Gasparini, F.; Fischer, U. C.; Buck, A. J. *Nucl. Med.* **2007**, *48*, 247.
- (11) Hintermann, S.; Vranesic, I.; Allgeier, H.; Bruelisauer, A.; Hoyer, D.; Lemaire, M.; Moenius, T.; Urwyler, S.; Whitebread, S.; Gasparini, F.; Auberson, Y. P. *Bioorg. Med. Chem.* **2007**, *15*, 903.
- (12) Burger, C.; Deschwanden, A.; Ametamey, S.; Johayem, A.; Mancosu, B.; Wyss, M.; Hasler, G.; Buck, A. *Nucl. Med. Biol.* **2010**, *37*, 845.
- (13) Calcinaghi, N.; Jolivet, R.; Wyss, M. T.; Ametamey, S. M.; Gasparini, F.; Buck, A.; Weber, B. J. *Cereb. Blood Flow Metab.* **2011**, *31*, e1.
- (14) DeLorenzo, C.; Kumar, J. S. D.; Mann, J. J.; Parsey, R. V. J. *Cereb. Blood Flow Metab.* **2011**, *31*, 2169.
- (15) Deschwanden, A.; Karolewicz, B.; Feyissa, A. M.; Treyer, V.; Ametamey, S. M.; Johayem, A.; Burger, C.; Auberson, Y. P.; Sovago, J.; Stockmeier, C.; Buck, A.; Hasler, G. *Am. J. Psychiatry* **2011**, *168*, 727.
- (16) Ouattara, B.; Gregoire, L.; Morissette, M.; Gasparini, F.; Vranesic, I.; Bilbe, G.; Johns, D. R.; Rajput, A.; Hornykiewicz, O.; Rajput, A. H.; Gomez-Mancilla, B.; Paolo, T. D. *Neurobiol. Aging* **2011**, *32*, 1286.
- (17) Treyer, V.; Streffer, J.; Wyss, M. T.; Bettio, A.; Ametamey, S. M.; Fischer, U.; Schmidt, M.; Gasparini, F.; Hock, C.; Buck, A. J. *Nucl. Med.* **2007**, *48*, 1207.
- (18) Wyss, M. T.; Ametamey, S. M.; Valerie, T.; Andrea, B.; Blagoev, M.; Kessler, L. J.; Burger, C.; Weber, B.; Schmidt, M.; Gasparini, F.; Alfred, B. *NeuroImage* **2007**, *35*, 1086.
- (19) Bruno, V.; Ksiazek, I.; Battaglia, G.; Lukic, S.; Leonhardt, T.; Sauer, D.; Gasparini, F.; Kuhn, R.; Nicoletti, F.; Flor, P. J. *Neuropharmacology* **2000**, *39*, 2223.
- (20) Lüscher, C.; Huber, K. M. *Neuron* **2010**, *65*, 445.
- (21) Ohnuma, T.; Augood, S. J.; arai, H.; McKenna, P. J.; Emson, P. C. *Mol. Brain Res.* **1998**, *56*, 207.
- (22) Pilc, A.; Klodzinska, A.; Branski, P.; Nowak, G.; Palucha, A.; Szewczyk, B.; Tatarczynska, E.; Chojnacka-Wojcik, E.; Wieronska, J. M. *Neuropharmacology* **2002**, *43*, 181.
- (23) Cosford, N. D. P.; Tehrani, L.; Roppe, J.; Schweiger, E.; Smith, N. D.; Anderson, J.; Bristow, L.; Brodwin, J.; Jiang, X. H.; McDonald, I.; Rao, S.; Washburn, M.; Varney, M. A. *J. Med. Chem.* **2003**, *46*, 204.
- (24) Gasparini, F.; Lingenhohl, K.; Stoehr, N.; Flor, P. J.; Heinrich, M.; Vranesic, I.; Biollaz, M.; Allgeier, H.; Heckendorn, R.; Urwyler, S.; Varney, M. A.; Johnson, E. C.; Hess, S. D.; Rao, S. P.; Sacca, A. I.; Santori, E. M.; Velicelebi, G.; Kuhn, R. *Neuropharmacology* **1999**, *38*, 1493.
- (25) Chiamulera, C.; Epping-Jordan, M. P.; Zocchi, A.; Marcon, C.; Cottiny, C. C.; Tacconi, S.; Corsi, M.; Orzi, F.; Conquet, F. O. *Nat. Neurosci.* **2001**, *4*, 873.
- (26) Todd, P. K.; Mack, K. J.; alter, J. S. M. *Proc. Natl. Acad. Sci. U.S.A.* **2003**, *100*, 14374.
- (27) Wang, Q.; Walsh, D. M.; Rowan, M. J.; Selkoe, D. J.; Anwyl, R. J. *Neurosci.* **2004**, *24*, 3370.
- (28) Ossowska, K.; Konieczny, J.; Wardas, J.; Pietraszek, M.; Kuter, K.; Wolfarth, S.; Pilc, A. *Amino Acids* **2007**, *32*, 179.
- (29) Rouse, S. T.; Marino, M. J.; Bradley, S. R.; Awad, H.; Wittmann, M.; Conn, P. J. *Pharmacol. Ther.* **2000**, *88*, 427.
- (30) Brown, A. K.; Kimura, Y.; Zoghbi, S. S.; Simeon, F. G.; Liow, J. S.; Kreisl, W. C.; Taku, A.; Fujita, M.; Pike, V. W.; Innis, R. B. *J. Nucl. Med.* **2008**, *49*, 2042.
- (31) Shetty, H. U.; Zoghbi, S. S.; Simeon, F. G.; Liow, J. S.; Brown, A. K.; Kannan, P.; Innis, R. B.; Pike, V. W. *J. Pharmacol. Exp. Ther.* **2008**, *327*, 727.
- (32) Simeon, F. G.; Brown, A. K.; Zoghbi, S. S.; Patterson, V. M.; Innis, R. B.; Pike, V. W. *J. Med. Chem.* **2007**, *50*, 3256.
- (33) Barret, O.; Tamagnan, G.; Batis, J.; Jennings, D.; Zubal, G.; Russell, D.; Marek, K.; Seibyl, J. J. *Nucl. Med. Meet. Abstr.* **2010**, *51*, 215.
- (34) Hamill, T. G.; Krause, S. R. C.; Bonnefous, C.; Govek, S.; Seiders, T. G.; Cosford, N. P. D.; Roppe, J.; Kamenecka, T.; Patel, S.; Gibson, R. E.; Sanabria, S.; Riffel, K.; Eng, W.; King, C.; Yang, X.; Green, M. D.; O'Malley, S. S.; Hargreaves, R.; Burns, H. D. *Synapse* **2005**, *56*, 205.
- (35) Baumann, C. A.; Mu, L.; Wertli, N.; Kramer, S. D.; Honer, M.; Schubiger, P. A.; Ametamey, S. M. *Bioorg. Med. Chem.* **2010**, *18*, 6044.
- (36) Honer, M.; Stoffel, A.; Kessler, L. J.; Schubiger, P. A.; Ametamey, S. M. *Nucl. Med. Biol.* **2007**, *34*, 973.
- (37) Lucatelli, C.; Honer, M.; Salazar, J. F.; Ross, T. L.; Schubiger, P. A.; Ametamey, S. M. *Nucl. Med. Biol.* **2009**, *36*, 613.
- (38) Sephton, S. M.; Dennler, P.; Leutwiler, D.; Mu, L.; Schibli, R.; Krämer, S. D.; Ametamey, S. M. *Chimia* **2012**, *66*, 201.
- (39) Sephton, S. M.; Dennler, P.; Leutwiler, D.; Mu, L.; Wanger-Baumann, C. A.; Schibli, R.; Krämer, S. D.; Ametamey, S. M. *Am. J. Nucl. Med. Mol. Imaging* **2012**, *2*, 14.
- (40) Baumann, C. A.; Mu, L.; Johannsen, S.; Honer, M.; Schubiger, P. A.; Ametamey, S. M. *J. Med. Chem.* **2010**, *53*, 4009.
- (41) Wanger-Baumann, C. A.; Mu, L.; Honer, M.; Belli, S.; Alf, M. F.; Schubiger, P. A.; Kramer, S. D.; Ametamey, S. M. *NeuroImage* **2011**, *56*, 984.
- (42) Fowler, J. S.; Volkow, N. D.; Wang, G. J.; Ding, Y. S.; Dewey, S. L. *J. Nucl. Med.* **1999**, *40*, 1154.
- (43) Reichel, A. *Chem. Biodivers.* **2009**, *6*, 2030.
- (44) Wilson, A. A.; Jin, L.; Garcia, A.; DaSilva, J. N.; Houle, S. *Appl. Radiat. Isot.* **2001**, *54*, 203.
- (45) Kirsch, P. *Modern fluoroorganic chemistry: synthesis, reactivity, applications*; Wiley-VCH: Germany, 2004.
- (46) Stavber, S.; Jereb, M.; Zupan, M. *Synthesis* **2002**, *17*, 2609.
- (47) Stavber, S.; Zupan, M. *Tetrahedron Lett.* **1996**, *37*, 3591.
- (48) Perkins, J. R.; Carter, R. G. *J. Am. Chem. Soc.* **2008**, *130*, 3290.
- (49) Differding, E.; Ofner, H. *Synlett* **1991**, 187.
- (50) Poss, A. J.; Shia, G. A. *Tetrahedron Lett.* **1995**, *36*, 4721.
- (51) Beeson, T. D.; MacMillan, D. W. C. *J. Am. Chem. Soc.* **2005**, *127*, 8826.
- (52) Marigo, M.; Fielenbach, D.; Braunton, A.; Kjaersgaard, A.; Jorgensen, K. A. *Angew. Chem., Int. Ed.* **2005**, *44*, 3703.
- (53) Steiner, D. D.; Mase, N.; C., F. B., III. *Angew. Chem., Int. Ed.* **2005**, *44*, 3706.
- (54) Kwiatkowski, P.; Beeson, T. D.; Conrad, J. C.; MacMillan, D. W. C. *J. Am. Chem. Soc.* **2011**, *133*, 1738.
- (55) Denmark, S. E.; Dappen, M. S. *J. Org. Chem.* **1984**, *49*, 798.
- (56) Collet, A.; Brienne, M. J.; Jacques, J. *Chem. Rev.* **1980**, *80*, 215.
- (57) Perez-Garcia, L.; Amabilino, D. B. *Chem. Soc. Rev.* **2007**, *36*, 941.
- (58) Sephton, M. A.; Emerson, C. R.; Zakharov, L. N.; Blakemore, P. R. *Chem. Commun.* **2010**, *46*, 2094.
- (59) Pan, Y. H.; Stothers, J. B. *Can. J. Chem.* **1967**, *45*, 2943.
- (60) Teare, H.; Robins, E. G.; Arstad, E.; Luthra, S. K.; Gouverneur, V. *Chem. Commun.* **2007**, 2330.
- (61) Chavan, S. P.; Thakkar, M.; Jogdand, G. F.; Kalkote, U. R. *J. Org. Chem.* **2006**, *71*, 8986.
- (62) Lin, J.; Nikaido, M. M.; Clark, G. J. *Org. Chem.* **1987**, *52*, 3745.
- (63) Murray, L. M.; O'Brien, P.; Taylor, R. J. K. *Org. Lett.* **2003**, *5*, 1943.
- (64) Thompson, C. F.; Jamison, T. F.; Jacobsen, E. N. *J. Am. Chem. Soc.* **2000**, *122*, 10482.
- (65) Pretsch, E.; Clerc, J. T.; Seibl, J.; Simon, W. *Tabellen zur strukturaufklärung organischer verbindungen mit spektroskopischen methoden*; Springer: Berlin, 1976; Vol. 15.
- (66) Stothers, J. B. *Carbon-13 NMR spectroscopy*; Academic Press: New York, 1972; Vol. 24.

NOTE ADDED AFTER ASAP PUBLICATION

This manuscript was published ASAP on August 9, 2012. Due to a production error, additional corrections were made to Table 1 and the revised version was reposted on August 14, 2012.